Schnase, J. L., M. L. Carroll, P. M. Montesano, and V. A. Seamster. 2024. Complex changes in climatic suitability for Cassin's Sparrow (*Peucaea cassinii*) revealed by retrospective ecological niche modeling. Journal of Field Ornithology 95(1):9. https://doi.org/10.5751/JFO-00432-950109

Avian Conservation and Management

Complex changes in climatic suitability for Cassin's Sparrow (*Peucaea cassinii*) revealed by retrospective ecological niche modeling

Cambios complejos en la idoneidad climática para el Gorrión de Cassin (*Peucaea cassinii*) revelados por modelado retrospectivo de nicho ecológico

John L. Schnase[1,2], *Mark L. Carroll*[1], *Paul M. Montesano*[1,2] *and Virginia A. Seamster*[3]

ABSTRACT. Conservation status assessments for Cassin's Sparrow (*Peucaea cassinii*) show considerable variability across the species' North American range. In this study, we combine data from NASA's Modern-Era Reanalysis for Research and Applications, Version 2 (MERRA-2; M2) with field observations spanning the past 40 years to investigate Cassin's Sparrow's response to multi-decadal changes in climatic suitability that could help explain this variability. We examine two time- and variable-specific time series using MaxEnt. The M2 time series uses a mix of microclimatic and ecosystem functional attributes; the MERRAclim-2 (MC) time series uses MERRA-2-derived bioclimatic variables. Trend analysis reveals complex patterns of slowly increasing climatic suitability over 69.5% of the study area in the MC time series accompanied by decreases over 24.4% of the area. Shifts in the study area–wide weighted centroid for suitability show a northwesterly, 40-year displacement of 1.85 km/yr. The M2 time series indicates a less favorable history with increasing and decreasing trends over 54.9% and 40.1% of the study area, respectively, and a westerly centroid shift of 2.60 km/yr. Increasing winds, drying land surface conditions, and variability in North American monsoon rainfall appear to be dominating, climate-related influences on the species. These variables also demonstrate complex patterns of non-constant spatial and temporal trends across the study area. We conclude that modeled estimates of climatic suitability for Cassin's Sparrow can vary widely depending on the temporal frame, spatial extent, and environmental drivers considered; that the species' response to non-constant trends in key environmental drivers is a potential source of this variability; that this variability mirrors the inconsistencies seen in the literature regarding the species' conservation status; and that retrospective ecological niche modeling that combines time and variable specificity, as we have done here, can be a useful adjunct to assessments of a species' conservation status.

RESUMEN. Las evaluaciones del estado de conservación del Gorrión de Cassin (*Peucaea cassinii*) muestran una variabilidad considerable en toda la distribución de la especie en América del Nore. En este estudio, combinamos datos del Reanálisis Retrospectivo de la Era Moderna para Investigación y Aplicaciones, Versión 2 (MERRA-2; M2 por sus siglas en inglés) de la NASA con observaciones de campo que abarcan los últimos 40 años, para investigar la respuesta del Gorrión de Cassin a los cambios de varias décadas en la idoneidad climática que podrían ayudar a explicar esta variabilidad. Examinamos dos series temporales de variables específicas utilizando MaxEnt. La serie temporal M2 utiliza una combinación de atributos funcionales micro climáticos y ecosistémicos; la serie temporal MERRAclim-2 (MC) utiliza variables bioclimáticas derivadas de MERRA-2. El análisis de tendencias revela patrones complejos de idoneidad climática que aumentan lentamente en más del 69.5% del área de estudio en la serie temporal MC, acompañado de disminuciones en más del 24.4% del área. Los desplazamientos en el centroide ponderado del área de estudio para determinar la idoneidad muestran un desplazamiento de 1.85 km/año hacia el noroeste durante 40 años. La serie temporal M2 indica una historia menos favorable con tendencias crecientes y decrecientes en 54.9% y 40.1% del área de estudio, respectivamente, y un desplazamiento del centroide hacia el oeste de 2.60 km/año. El aumento de los vientos, la sequía de la superficie terrestre y la variabilidad en las precipitaciones monzónicas de América del Norte parecen ser influencias dominantes relacionadas con el clima sobre la especie. Estas variables también demuestran patrones complejos de tendencias espaciales y temporales no constantes en toda el área de estudio. Concluimos que las estimaciones modeladas de idoneidad climática para el Gorrión de Cassin pueden variar ampliamente dependiendo del marco temporal, la extensión espacial y los factores ambientales considerados; que la respuesta de la especie a tendencias no constantes en los factores ambientales clave es una fuente potencial de esta variabilidad; que esta variabilidad refleja las inconsistencias observadas en la literatura respecto al estado de conservación de la especie; y que el modelado de nicho ecológico retrospectivo que combina el tiempo y la especificidad variable, como hemos hecho aquí, puede ser un útil complemento para las evaluaciones del estado de conservación de una especie.

Key Words: *conservation status assessments; MERRA-2; MERRAclim-2; non-stationarity; Theil-Sen trend analysis; time-specific ENM; variable-specific ENM*

INTRODUCTION

Cassin's Sparrow's environmental preferences

Cassin's Sparrow (*Peucaea cassinii*, Woodhouse 1852) is a small, gray, ground-dwelling endemic of the arid grasslands of the southwestern United States (U.S.) and northern Mexico (Woodhouse 1852, Williams and LeSassier 1968, Dunning et al. 2020). It is migratory, constructs nests near the ground, and is notable for its secretive nature and highly developed flight song. Studies have shown that Cassin's Sparrow's behavioral ecology is closely linked to wide-spread, seasonal weather patterns as well as highly localized, ground-level climatic conditions (Williams and LeSassier 1968, Schnase et al. 1991, Ruth 2000, Dunning et al. 2020). Regional precipitation appears to be of particular importance at the macroclimatic scale, presumably due to its influence on vegetation availability and insect abundance. In fact, field studies over the past century suggest that Cassin's Sparrow is an itinerant breeder, so responsive to regional rainfall patterns that birds make seasonal, inter-clutch moves within their range to find optimal conditions for breeding (Williams and LeSassier

[1]NASA Goddard Space Flight Center, [2]ADNET Systems, Inc., [3]New Mexico Department of Game and Fish

1968, Ohmart 1969, Dunning et al. 2020). At the microclimatic scale, wind speed and ambient temperature are important influences. In a behavior that is uncommon among North American birds, male Cassin's Sparrows defend territories and secure mates using aerial flight song displays. Elevated winds and temperatures reduce the birds' capacity to perform this energetically demanding skylarking behavior, which is an essential element of the species' breeding biology (Schnase and Maxwell 1989, Schnase et al. 1991).

Although much of what is reported about the natural history of Cassin's Sparrow is poorly established, Cassin's Sparrow's apparent responsiveness to environmental conditions raises a concern that the species could be among the many North American grassland birds that are vulnerable to climate change (Schnase et al. 1991, Ruth 2000, Wilsey et al. 2019, Dunning et al. 2020). Accurate range-wide assessments, however, are often difficult with these species (Hubbard 1974, Huntley et al. 2010, Reside et al. 2010, Heenan and Seymour 2012, Sohl 2014, Lipschutz 2016, Norman and Christidis 2016, Iknayan and Beissinger 2018, Rosenberg et al. 2019). With Cassin's Sparrow, for example, numerous studies over the past half-century have painted an inconsistent picture. Some studies find evidence for a retraction of viable habitat and declining populations across North America (Lynn 2006; North American Breeding Bird Survey, https://www.pwrc.usgs.gov/bbs/), whereas others find mixed results and too little data to establish with confidence an overall status (Ruth 2000). Many sources identify the species as stable and of low conservation concern (Rosenberg et al. 2016, Dunning et al. 2020; National Audubon Society, https://www.audubon.org; NatureServe, https://explorer.natureserve.org). State-level studies are often no more definitive. The State Wildlife Action Plan for New Mexico, for example, lists Cassin's Sparrow as a declining species, susceptible to shifting environmental conditions that could lead to rapid population changes (New Mexico Department of Game and Fish 2016). At the same time, of nine grassland birds in New Mexico, recent work has shown Cassin's Sparrow to be the only species for which gains in suitable habitat are projected over the next 50 years (Salas et al. 2017).

These differing views of Cassin's Sparrow's status suggest that a fundamental aspect of the species' relationship to the environment is not well understood. From first principles, we know that the multidimensional niche space of a species may shift, through adaptation or acclimation, as may its demography in response to climate changes (Maguire 1973). We also know that climate change can drive shifts in the spatial distribution of many bird species as they track suitable conditions (Pecl et al. 2017). In addition, recent work underscores the importance of non-constant processes, such as long-term trends, seasonal or temporal cycles, or random variation, which can cause climatic drivers to vary in complex ways over time and space, a phenomenon referred to as non-stationarity (Rollinson et al. 2021, Ward et al. 2022). It is generally agreed that the most important contemporary driver of non-stationary environmental trends is global climate change (Ward et al. 2022).

Past response to a changing climate can offer insights

Cassin's Sparrow's past response to a changing climate could help explain the variability we see in the species' status assessments as well as the underlying biological mechanisms for this response. This is especially true if macro- and microclimatic patterns vary across Cassin's Sparrow's range and the variability among these assessments arises from the species' response to non-constant trends in key environmental drivers. Ecological niche modeling (ENM) is a set of techniques and tools that is often used in this type of research. ENM uses species occurrence records and environmental data to estimate the probabilities of suitable habitats across a study area (Peterson et al. 2011). Although ENM is commonly used to project future responses of a species to climatic change, less consideration has been given to historical responses to a changing climate that could shed light on core biological questions or the present and future status of a species (Johnston et al. 2020). In this study, we combine data from NASA's Modern-Era Reanalysis for Research and Applications, Version 2 (MERRA-2; M2) with field observations spanning the past 40 years to perform a retrospective ENM analysis of Cassin's Sparrow's evolving climatic niche to help answer three questions that bear on this issue:

1. How has Cassin's Sparrow responded to changing climatic conditions in the past?
2. What are the specific attributes of climatic change that the species is responding to?
3. Could Cassin's Sparrow's response to changing climatic conditions account for the variability seen in assessments of the species' conservation status?

To address the first question, we use changing historical patterns of climatic suitability as an indirect indicator of the species' response to changing conditions. For the second question, we use changes in the types of predictors of climatic suitability over time to identify the key attributes driving Cassin's Sparrow's biological response. To gain a perspective on the third question, we look at changing patterns in the values of key predictors over time to gauge their potential as a source of variability.

Retrospective ENM's three-element approach

To address these questions, we have taken an approach that embodies a novel integration of three elements. First, we base our analysis on environmental variables obtained solely from the M2 reanalysis. Climate reanalyses combine past observations with numerical models to generate a consistent time series of hundreds of fundamental, physical drivers of the Earth system. They offer a comprehensive description of Earth's observed climate as it has evolved over the past half century at a fine temporal scale (Edwards 2010). The current study spans the 40-year period from 1980 to 2019 and is based on two climatic variable time series. In one time series, we use 30 M2 variables selected to reflect key attributes of the microclimate that are known to relate directly or indirectly to the biological or ecological functioning of a species. This collection of predictors is intended to help us understand the influence of climate-related conditions in localized areas near the Earth's surface and includes variables, such as temperature near and on the ground, humidity, wind speed, cloud cover, soil moisture, evapotranspiration, vegetation coverage, and the incoming and reflected solar radiation that provides energy to drive ecosystem functioning at the micro scale (Schnase et al. 1991, Cabello et al. 2012, Bosilovich et al. 2016, Gelaro et al. 2017, Arenas-Castro et al. 2018, Pettorelli et al. 2018, Regos et al. 2022a, 2022b). In the second time series, we use 19 M2-derived bioclimatic variables modeled after the classic bioclim predictors

commonly used in ENM (O'Donnell and Ignizio 2012). This collection of predictors is intended to help us understand the influence of wide-spread, yearly, seasonal, and monthly temperature and precipitation patterns. Together, these two sets of predictors provide a more detailed view of macro- and microclimatic factors influencing environmental suitability for Cassin's Sparrow than could be realized by using either set of predictors alone.

Second, we employ time-specific ENM in our analysis: our dependent and independent variables are temporally aligned across the time span of the study. Detailed information about the geographic distribution and changing dynamics of climatic suitability for a species is critical to conservation planning (Guisan et al. 2013, Porzig et al. 2014, Gonçalves et al. 2016, Rollinson et al. 2021). ENM is often applied within a time-averaged framework in which the values of environmental variables are averaged over time spans that are not in temporal registration with the occurrence records upon which models are calibrated or tested (Bede-Fazekas and Somodi 2020, Ingenloff and Peterson 2021). Although useful for exploring species distributions at a broad level, modeling within a time-averaged framework can elide complex effects of the environment on an organism, especially highly mobile or behaviorally complex species (Roubicek et al. 2010, Ingenloff 2020). Of particular concern to conservation work, studies have shown that temporal mismatches in the time period spanned by occurrence data and the climate baseline can decrease the utility and accuracy of ENM products (Roubicek et al. 2010, Goberville et al. 2015, Guida et al. 2019, Pérez-Navarro et al. 2021). In this work, we use five-year averaged values for our environmental variables across a sequence of eight time intervals spanning the 40-year period of the study. We then use time-specific species observations corresponding to these five-year intervals as dependent variables in the models that form the basis of our analyses, thereby enabling a temporally explicit view into the major, range-wide, historical patterns of changing climatic suitability for Cassin's Sparrow.

Finally, we employ variable-specific ENM in our analysis: a tailored set of independent variables is used for each of the five-year intervals in the time series. ENM generally uses a fixed set of variables in a given study. These variables are typically selected through a manual process based on an ecological understanding of the species being studied or one of a variety of statistical approaches (Petitpierre et al. 2017). However, retrospective ENM using reanalysis data presents an opportunity to examine changes in the drivers of climatic suitability themselves over time. In this study, we use NASA's MERRA/Max system to perform automatic variable screening within each of the five-year time intervals of the analysis. MERRA/Max provides a scalable feature selection approach that enables direct use of global climate model (GCM) outputs in ENM (Schnase and Carroll 2022). The system accomplishes this selection through a Monte Carlo optimization that screens a collection of variables for potential predictors of suitable conditions (Schnase et al. 2021). With MERRA/Max, variable selection is guided by the indirect biological influences injected into the algorithm's selection process by the species occurrence files, identifying biologically and ecologically plausible predictors in large, multidimensional data sets where selection through ecological reasoning or other means is not feasible (Searcy and Shaffer 2016, Smith and Santos 2020). Variable selection for each five-year time interval, as applied here, enables a view into the changing patterns of environmental determinants of climatic suitability that would otherwise be difficult, if not impossible, to obtain. That view, in turn, provides a way of examining the possible underlying biological basis for Cassin's Sparrow's response to a changing climate.

Collectively, these three aspects of the study offer a more detailed look at Cassin's Sparrow's relationship to the environment than has been previously reported. In the sections that follow, we describe our method and results, discuss what we see as the important takeaway lessons from the study, and conclude with recommendations for next steps.

METHODS

Modeling environment and study approach

We framed the study as an analysis of broad-scale, multi-decadal changes in the climatic suitability for Cassin's Sparrow. To that end, we did not focus on changes in the species' range, population size, or abundance, and, in the current work, we do not look at higher temporal resolution or inter-annual trends in climatic suitability, which would have added significantly to the computational burden of the analysis. We used MaxEnt for our modeling environment (Phillips et al. 2006, Elith et al. 2011, Phillips et al. 2017). Based on a machine learning approach to maximum entropy modeling, MaxEnt calculates the distribution of suitable habitats using species occurrence data and a set of environmental variables (Phillips et al. 2006, 2017, Elith et al. 2011, Merow et al. 2013, Kalinski 2019). The system uses presence data only, comparing the locations of where a species has been found to environmental data from across the study region. MaxEnt defines the overall environment by sampling a large number of background points throughout the region, including locations where the species is known to occur as well as locations where the species' presence or absence is unknown. Background points are intended to be so numerous that they capture the full environmental space of the study area and, importantly, so outnumber the occurrence locations that favorable conditions for a species can be mathematical distinguished from the overall environmental context. MaxEnt produces accurate predictions with even small sample sizes and often produces better results when the number of presence locations is reduced by statistical thinning or filtered in an ecologically meaningful way (Pearson et al. 2007, Boria et al. 2014, Aiello-Lammens et al. 2015, Phillips et al. 2017).

Preparing species occurrence data

We used annual, time-stamped, point locations for Cassin's Sparrow occurrences across the species' full North American range, making no distinction between breeding and non-breeding season observations. We obtained occurrence data from the Global Biodiversity Information Facility (GBIF, https://www.gbif.org), an international information infrastructure funded by the world's governments that provides open access to data about all types of life on Earth. Occurrence datasets make up the core of what is published by GBIF. GBIF's standardized formatting, documentation, and quality requirements are enforced through close collaboration with data providers. We downloaded a total of 32,518 records for the years 1980 to 2019 (GBIF occurrence

Fig. 1. Workflow showing the major processing steps used in the study: (A) data preparation, (B) time series construction, and (C) time series analysis. Data sources include the Global Biodiversity Information Facility (GBIF) and the Goddard Earth Sciences Data and Information Services Center (GES DISC).

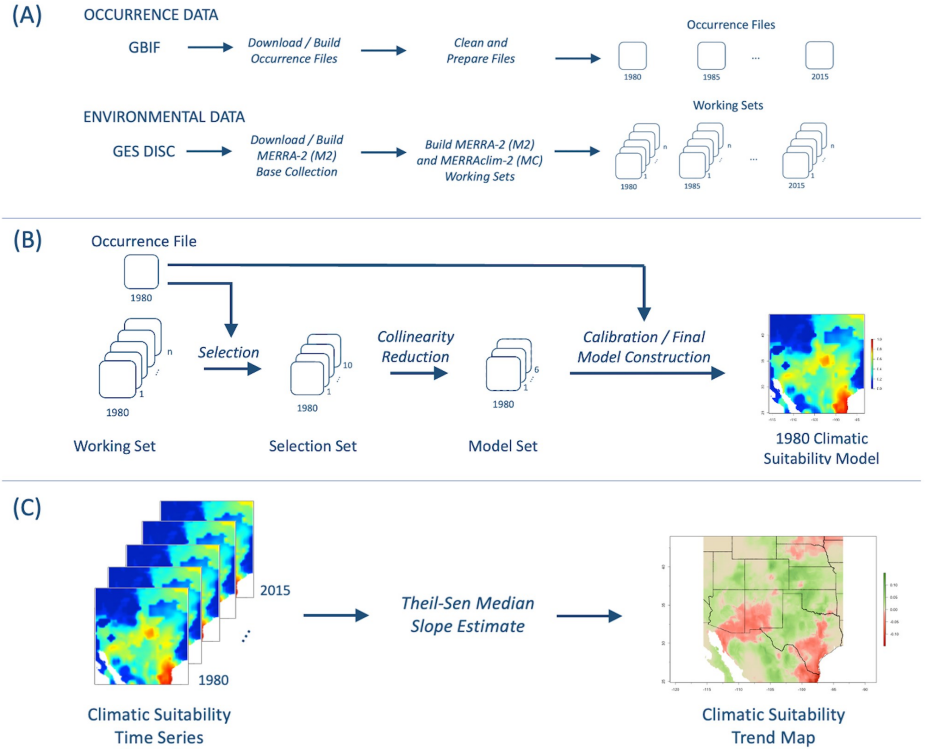

download, https://doi.org/10.15468/dl.x33grq [15 January 2022]). More than 95% of the records were originally sourced from the eBird citizen-scientist observational dataset (https://ebird.org/species/casspa), but the download also included research-grade records from iNaturalist (https://www.inaturalist.org), the National Ecological Observational Network's breeding land bird point count collection (https://www.neonscience.org), and museum specimen records from the National Museum of Natural History (https://naturalhistory.si.edu), American Museum of Natural History (https://www.amnh.org), Harvard University's Museum of Comparative Zoology (https://mcz.harvard.edu), Kansas University Biodiversity Institute and Natural History Museum (https://biodiversity.ku.edu), and the University of Arizona Museum of Natural History (https://www.arizonamuseumofnaturalhistory.org).

There were relatively few occurrence records in the early years of the study's time span. We found that binning records into five-year intervals gave us enough observations to produce useful models across the long time period of the study. We therefore merged the GBIF observations into a time-series comprising eight, five-year aggregated collections: 1980–1984, 1985–1989, 1990–1994, 1995–1999, 2000–2004, 2005–2009, 2010–2014, and 2015–2019 (Fig. 1A). These five-year collections initially ranged in size from 263 records in the 1980 group to over 14,000 records in the 2015 collection. After removing replicates, we thinned the records to non-overlapping observations within a 16 km (~10 mile) buffer around each point to avoid double counting the same individuals. For count uniformity across the series and to reduce record-densities that can diminish model performance, we extracted random 250-record samples for each five-year span in the time series (Boria et al. 2014). In trials using various sample sizes, we found that 250 records per five-year interval yielded the most consistently accurate models across the 40-year time series.

Preparing environmental variables

We created two sets of environmental variables for the analysis. We began by defining a study area that encompasses Cassin's Sparrow's summer and winter ranges across the Continental U. S. using information from the U.S. Geological Survey (USGS) National Gap Analysis Program (GAP) (https://doi.org/10.5066/F7Q81B3R). We selected a study area that extended from latitude 24.8° N to 44.0° N and longitude 93.5° W to 115.6° W. We then obtained a base collection of maximum, minimum, and mean values of 30 gridded M2 variables across our spatial and temporal domain, natively available from NASA's Goddard Earth Sciences Data and Information Services Center (https://disc.gsfc.nasa.gov; Table 1, Fig. 1A). This collection contained the precursor temperature and precipitation variables from which the 19 classic, bioclim predictors used in ENM are derived (O'Donnell and Ignizio 2012). In addition, it included environmental attributes of more direct biological significance that are not explicitly represented in the 19 traditional bioclimatic variables, such as soil moisture and evaporation from land, wind direction and speed, and various solar radiation fluxes. We aggregated these data to our five-year time intervals to create working set collections of

Table 1. MERRA-2 (M2) variables.

Variable	Description[1]
TS	Surface skin temperature (K)
QV2M	2-meter specific humidity (kg/kg)
T2M	2-meter air temperature (K)
EFLUX	Positive latent heat flux (W/m^2)
HFLUX	Positive sensible heat flux (W/m^2)
SPEED	Surface wind speed (m/s)
PREVTOT	Total re-evaporation/sublimation of precipitation ((kg/m^2)/s)
PRECTOTCORR	Total observation-corrected surface precipitation ((kg/m^2)/s)
ALBEDO	Surface albedo
LWGNT	Surface net downward longwave flux (W/m^2)
SWGNT	Surface net downward shortwave flux (W/m^2)
TAUTOT	Optical thickness of all clouds
CLDTOT	Total cloud area fraction
LAI	Leaf area index
GRN	Vegetation greenness fraction (LAI-weighted)
GWETPROF	Average profile soil wetness
GWETROOT	Root zone soil wetness
TSURF	Mean land surface temperature (K)
TSAT	Surface temperature of saturated zone (K)
FRWLT	Fractional wilting area
QINFIL	Soil water infiltration rate ((km/m^2)/s))
GHLAND	Downward heat flux into topsoil layer (W/m^2)
WCHANGE	Total land water change per unit time ((kg/m^2)/s)
ECHANGE	Total land energy change per unit time (W/m^2)
PRMC	Total profile soil moisture content (m^3/m^3)
RZMC	Root zone soil moisture content (m^3/m^3)
EVPSOIL	Bare soil evaporation energy flux (W/m^2)
EVPTRNS	Transpiration energy flux (W/m^2)
EVPINTR	Interception loss energy flux (W/m^2)
EVLAND	Evaporation from land ((kg/m^2)/s)

[1] See Appendix A for a more detailed description of the M2 variables.

Table 2. MERRAclim-2 (MC) variables.

Variable	Description
MC_Bio01	Annual mean temperature (°C)
MC_Bio02	Mean diurnal temperature range (°C)
MC_Bio03	Isothermality [(MC_Bio02/MC_Bio07)*100] (%)
MC_Bio04	Temperature seasonality [(Standard deviation*100)] (°C)
MC_Bio05	Maximum temperature of the warmest month (°C)
MC_Bio06	Minimum temperature of the coldest month (°C)
MC_Bio07	Temperature annual range (MC_Bio05-MC_Bio06) (°C)
MC_Bio08	Mean temperature of the wettest quarter (°C)
MC_Bio09	Mean temperature of the driest quarter (°C)
MC_Bio10	Mean temperature of the warmest quarter (°C)
MC_Bio11	Mean temperature of the coldest quarter (°C)
MC_Bio12	Annual precipitation (mm)
MC_Bio13	Precipitation of the wettest month (mm)
MC_Bio14	Precipitation of the driest month (mm)
MC_Bio15	Precipitation seasonality (Coefficient of variation) (%)
MC_Bio16	Precipitation of the wettest quarter (mm)
MC_Bio17	Precipitation of the driest quarter (mm)
MC_Bio18	Precipitation of the warmest quarter (mm)
MC_Bio19	Precipitation of the coldest quarter (mm)

the five-year averaged mean values for each variable, which we then formatted for use by MaxEnt. To smooth the representation of local environmental conditions, we resampled the M2 layers from their native spatial resolution of 1/2° latitude × 5/8° longitude to 5.0 arc-min (1/12°) resolution (~7.6 km at latitude 35.0° N) using bilinear interpolation. We also built working set collections of M2-derived bioclimatic variables, one set per five-year interval, which we refer to as the MERRAclim-2 (MC) working set collection (Table 2). These were modeled after Worldclim's 19 bioclim variables; however, because the classic Worldclim collection is based on 30-year averaged values, we created an M2-based version to accommodate the time-specificity requirement of the study. For this, we used the R dismo library following the method of Vega et al. (Vega et al. 2017, Hijmans et al. 2023). We employed M2's monthly maximum and minimum temperature values (T2M) and the averaged values for monthly precipitation (PRECTOTCORR) to create the MC working set collections, which conveyed the added consistency of MC's 19 variables being derived from the same data sources as M2.

Building the time series

We built two MaxEnt climatic suitability time series using the aggregated GBIF occurrence collections. In one, we used the M2 working sets as independent variables; in the other, we used the MC working sets as independent variables. A two-step processing workflow was applied to each five-year interval of each time series (Fig. 1B).

Selecting and refining time-specific variables

First, we used MERRA/Max to automatically select top contributing M2 and MC variables in each of the eight, five-year spans of the 40-year series. We performed three screening runs, each returning a set of top ten selected variables using MERRA/Max's standard screening configuration and a per-variable sampling rate of 100 (Schnase and Carroll 2022). We averaged the results of the three runs to create a selection set of the top ten predictors for each five-year interval. We then used variance inflation factor (VIF) analysis to reduce collinearities in the selected predictors (Pradhan 2016). This resulted in a final, model set of top predictors for each five-year interval in the two time series that had few if any collinearity issues.

Calibrating and building time-specific models

Next, we built calibrated models for each set of occurrences and predictors in each of the five-year intervals in the M2 and MC time series. We used the R ENMeval package to identify optimal MaxEnt parameter settings for each interval (Muscarella et al. 2014, Kass et al. 2023). ENM automatically creates a collection of models across a range of settings and uses Akaike's Information Criterion corrected for small sample size (AICc; Akaike 1974) to measure information loss among the models. The combination of MaxEnt parameter settings that results in the lowest AICc value is taken to be an optimal tuning configuration for a given set of inputs. We used these optimal settings to construct a final model for each five-year interval in the two time series. For each of the ENMeval calibration runs, and in the final MaxEnt model run, we used 10,000 background locations randomly selected from across the study area and performed a 10-fold cross validation in which 70% of the occurrences were selected for training and 30% for testing in each repetition (Phillips et al. 2017). Cloglog format was used throughout. This model calibration and construction process was performed in triplicate for each five-year interval to produce the final models that we used in the subsequent time series analysis.

Analyzing time series results

We analyzed our time series results by creating trend maps showing regions of positive and negative change in climatic suitability per five-year interval across the study area over the 40-year span of the study (Fig. 1C). We used the Theil-Sen median slope estimate to build these trend maps. Theil-Sen provides a non-parametric means of robustly fitting a line to a set of points by finding the median slope of all the lines through all pairs of points in the set. In our case, the estimate was applied for each pixel across the eight raster layers comprising the final models of climatic suitability for each 40-year time series. There were, thus, eight points, one per five-year interval, in the slope calculation for each pixel in the resulting trend maps. We used Mann-Kendall Z values to determine the statistical significance of the resulting trends (Theil 1950, Sen 1968).

We then quantified the overall direction and speed of shifts in climatic suitability observed in the trend maps. We used the movement of weighted centroids to characterize these shifts. Weighted centroids represent the geometric center of all pixels in the studied area, weighted by their suitability index (VanDerWal et al. 2013). We chose weighted centroids for this purpose because of their ability to account for information derived from across a species' entire modeled range. We quantified movement by measuring length and direction of the vector between weighted centroids of the 1980 and 2015 probability maps.

Finally, we examined trends in the values of the most important variables across the time series. Top contributing variables were those that appeared in half or more of the 24 final models in the triplicated time series; these variables were ranked by their average permutation importance across the three runs (Searcy and Shaffer 2016). For the top, study-wide contributing variables, we computed Theil-Sen slopes to visualize patterns of change in the values of the M2 and MC variables across the study area. We then examined trends in the relative contributions (i.e., permutation importance) of each of these top variables per five-year interval across the 40-year span of the study.

The final models in both time series were qualitatively judged for reasonableness on the basis of first-hand knowledge of the species and its environmental preferences and what can be inferred about climatic contexts from published estimates of Cassin's Sparrow's North American range. We used the Area Under the Receiver Operating Characteristic (ROC) Curve (AUC; Fielding and Bell 1997), the True Skill Statistic (TSS; Allouche et al. 2006), and Percent Correctly Classified (PCC; Warren and Seifert 2011) as measures of model accuracy.

RESULTS

Evaluation of model performance

Our models exhibited moderate performance across the 24 final models in each triplicated time series according to their mean AUC, PCC, and TSS values (Table 3). In evaluating model performance, we regarded AUC measures < 0.7 as low, 0.7–0.9 as moderate, and > 0.9 as high; similarly, we regarded TSS and PCC measures < 0.5 as poor, 0.5–0.8 as useful, and > 0.8 as good (Arenas-Castro et al. 2018). The AICc estimate of information quality in the final models within and across the two time series was highly consistent. Against these metrics, we judged the observed level of performance to be a sufficient basis for examining the broad trend patterns displayed by the time series models, which was the primary focus of the study. The observed spatial distribution of suitable conditions corresponded well with what is known about the natural history of the species and published range maps.

Table 3. Overall model performance for the M2 and MC time series. Metrics include Area Under the Receiver Operating Characteristic (ROC) Curve (AUC), Percent Correctly Classified (PCC), True Skill Statistic (TSS), and Akaike's Information Criterion corrected for small sample size (AICc). Mean ± standard error used throughout, n = 24 in both time series.

Time series	AUC	PCC	TSS	AICc
M2	0.817 ± 0.009	0.718 ± 0.023	0.528 ± 0.017	1991.248 ± 27.345
MC	0.812 ± 0.007	0.734 ± 0.008	0.789 ± 0.020	1963.185 ± 23.849

Evaluation of suitability trends

Overall trends

The study area encompassed approximately 3.91 x 10^6 km². Broad areas of climatic suitability change across the study area were observed in both time series over the past 40 years. The most favorable climatic conditions for Cassin's Sparrow have generally concentrated in the southeastern regions of the study area according to both the M2 and MC time series; however, over time, a northwesterly shift in areas of high suitability is apparent in both series (Figs. 2A, 3A). The Theil-Sen trend maps also show a northwesterly movement in increasing climatic suitability over the past 40 years, although the patterns of change are more broadly diffuse in the M2 series, as described in greater detail below (Figs. 2B, 3B). An overall increase in climatic suitability was identified over approximately 54.9% of the study area (~21.49 x 10^5 km²) in the M2 time series and 69.5% of the study area (~27.21 x 10^5 km²) in the MC series (Table 4). Areas showing an overall decrease in climatic suitability ranged in size from approximately 40.1% (~15.72 x 10^5 km²) in the M2 time series to 24.4% of the study area (~9.54 x 10^5 km²) in the MC series.

Statistically significant trends

Areas of statistically significant change at the 95% confidence level are relatively small, and the rates of positive and negative change in those regions are low (Table 4). Theil-Sen results in the M2 series indicate that the estimated probabilities of climatic suitability have been increasing by an average of 0.03 every five years for the past 40 years across 6.2% of the study area, with a corresponding average decrease in estimated probabilities of 0.05 every five years over 0.5% of the region. Statistically significant positive trends were concentrated in the central, northwestern, and far southwestern regions of the study area, whereas statistically significant negative trends concentrated in the southeast and central southwest, imparting a west to northwesterly axis to these positive shifts that is consistent with the weighted centroid analysis, as described below.

Theil-Sen results for the MC time series paint a similar picture. Probability estimates of climatic suitability, within areas of statistically significant change, have been increasing by an average of 0.03 every five years for the past 40 years across 5.5% of the

Fig. 2. M2 climatic suitability trends showing the averaged results from three time series runs. (A) Estimated probabilities of climatic suitability for Cassin's Sparrow for each of the five-year intervals spanning 1980 to 2019. Probability values range from 0.0 to 1.0 with warmer colors indicating more favorable conditions. (B) Spatial distribution of Theil-Sen slopes showing the rate of change in probabilities of climatic suitability per five-year interval across the 40-year time series. Positive trends are indicated in green, negative trends in red. Statistically significant positive and negative trends at the 95% confidence level are shown in dark green and red, respectively. Colored outlines indicate the northern extent of Cassin's Sparrow's U.S. breeding (red) and non-breeding (blue) ranges. Cassin's Sparrow's summer, breeding range encompasses all of the species' winter, non-breeding range. The yellow box shows the location of a shift in weighted centroids for climatic suitability from 1980 (o) to 2015 (•).

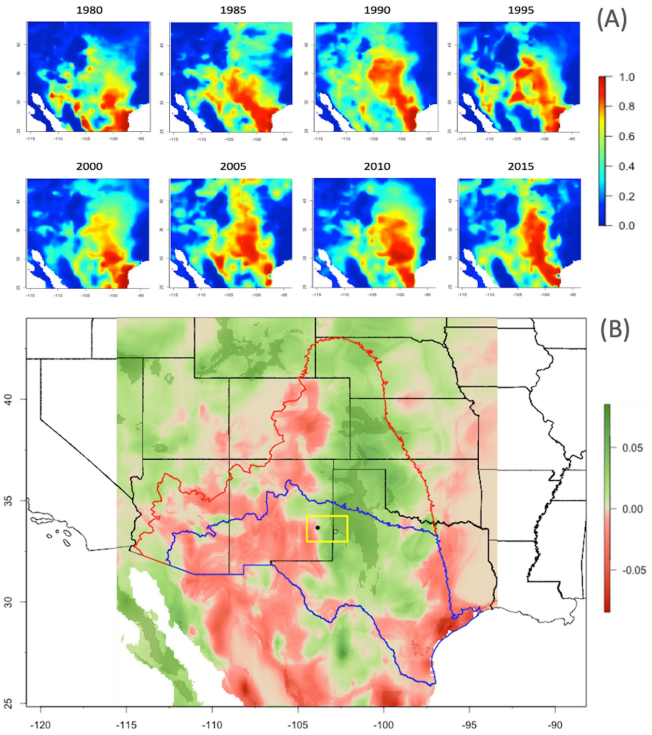

Fig. 3. MC climatic suitability trends showing the averaged results from three time series runs. See Figure 2 caption for additional detail.

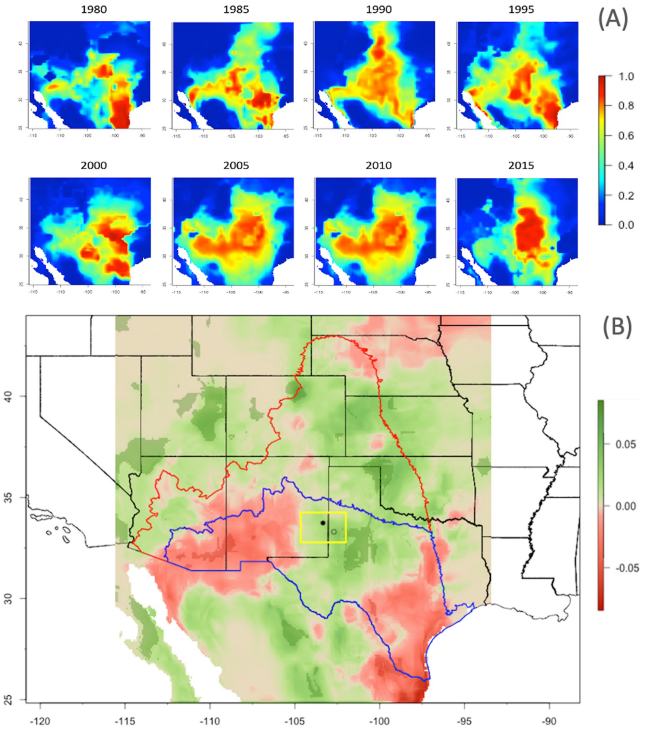

study area, with an accompanying average decrease in estimated probabilities of 0.06 every five years over 0.9% of the region (Table 4). Statistically significant positive trends concentrated in three clusters, one each in the northwest and northeast, the third in a central southwest region, which, by contrast, showed a negative trend in the M2 analysis. However, there was a statistically significant negative trend in the southeast region for the MC series that coincides with the pattern observed for the M2 series.

Patterns of climatic suitability shift

Overall shifts in the climatic suitability for Cassin's Sparrow were observed in both time series. The 40-year displacement of the weighted centroid for suitability in the M2 time series was approximately 104 km and had a westerly trajectory (282°). This pattern contrasted with that seen in the MC time series, which showed a 40-year displacement of 75 km along a northwesterly trajectory (309°; Fig. 4). Centroid movement in the M2 time series shows a higher change velocity than that seen in the MC time series (2.60 km/yr vs. 1.85 km/yr, respectively).

Evaluation of variable trends

Trends in the MERRA-2 (M2) predictors

Seven M2 variables appeared in more than half of the models in the M2 time series (Table 5). Each variable demonstrated complex patterns of non-constant spatial and temporal trends across the study area (Fig. 5), making it difficult to generalize about increasing or decreasing conditions. For example, Theil-Sen analysis showed generally positive trends across the study area for SPEED, QV2M, PREVTOT, and SWGNT, with positive change centrally located in the study area for SWGNT, concentrated in northern, northeastern, and southeastern regions for QV2M, and broadly scattered in SPEED and PREVTOT. Predominantly negative trends were seen in EVPSOIL and EVPINTR, with EVPSOIL's negative changes concentrated in the southwest and EVPINTR's broadly distributed across the entire study area. Nearly equivalent areas of overall positive and negative change were observed for TAUTOT (Table 6), with positive change concentrated in the north and southeast. The M2 trends generally lacked statistical significance.

Table 4. Theil-Sen median slope analysis of the study's two time series. Results are reported for the map regions in Figures 2B and 3B that exhibited change at any level of statistical significance (overall trends) as well as statistically significant change at the 95% confidence level (statistically significant trends). Results are based on the three trend maps produced by the triplicated runs in each time series and show mean ± standard error across these three maps. Positive (Pos) and negative (Neg) trends are indicated by the corresponding positive and negative Mann-Kendall Z scores (Z). Theil-Sen slope values (TS) represent the rate of change in estimated probabilities of climatic suitability per five-year interval across the 40-year time series in areas showing statistically significant trends.

Time series		Overall trends		Statistically significant trends			
		$km^2 \times 10^5$	% of area	Z	$km^2 \times 10^5$	% of area	TS Δ / 5-yr
M2	Pos	21.49 ± 3.96	54.9 ± 10.0	3.09 ± 0.01	2.41 ± 0.64	6.2 ± 1.6	0.03 ± 0.05
	Neg	15.72 ± 1.28	40.1 ± 3.2	−2.85 ± 0.15	0.19 ± 0.07	0.5 ± 0.2	−0.05 ± 0.01
MC	Pos	27.21 ± 1.07	69.5 ± 2.6	3.34 ± 0.08	2.15 ± 0.11	5.5 ± 0.3	0.03 ± 0.01
	Neg	9.54 ± 0.06	24.4 ± 2.7	−2.09 ± 0.01	0.37 ± 0.05	0.9 ± 0.1	−0.06 ± 0.02

Fig. 4. Maps showing the direction, distance, and velocity of 40-year shifts in the weighted centroids for climatic suitability for Cassin's Sparrow in (A) the M2 time series and (B) the MC time series from 1980 (o) to 2015 (•). For orientation, Roswell, New Mexico, is the city on the western boundary of the maps. Base map courtesy of the USGS with annotations by the authors.

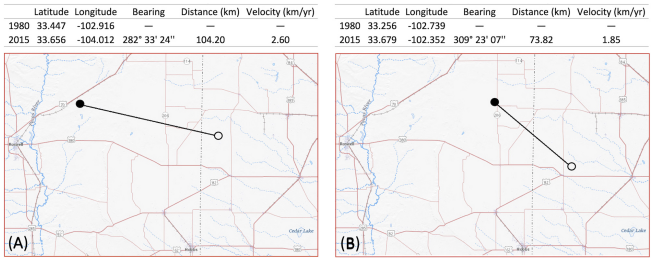

Trends in the MERRAclim-2 (MC) predictors

Seven MC variables also appeared in more than half of the models in the MC time series (Table 5). These variables demonstrated complex patterns of changing spatial and temporal trends across the study area as well (Fig. 5). Theil-Sen analysis showed predominantly positive trends across the study area for MC_Bio08, MC_Bio15, and MC_Bio05, with large expanses of positive change concentrated centrally and in the northwest region of the study area for MC_Bio05, concentrated in the southwest for MC_Bio08, the west and southwest for MC_Bio15. Negative trends dominated in MC_Bio14 and MC_Bio18, especially in the western half of the study area. Nearly equivalent areas of positive and negative change were seen in MC_Bio03 and MC_Bio13 (Table 6), with broadly scattered patches of change apparent for each variable throughout the study area. Most of the trends observed in the MC variables also lacked statistical significance.

Variable contribution trends across the time series

The relative importance of the top contributing variables also varied across the 40-year span of the study (Fig. 6). In the M2 time series, we observed a generally increasing trend in the contributions of EVPINTR to each five-year interval's final model and a generally decreasing trend in the contributions of QV2M and SWGNT. SPEED and EVPSOIL were consistently high contributors; TAUTOT and PREVTOT were consistently moderate contributors. In the MC series, MC_Bio14 and MC_Bio03 show generally increasing trends; MC_Bio08 showed a sharply decreasing trend. MC_Bio18 was a consistently high contributor, with MC_Bio15, MC_Bio05, and MC_Bio13 making consistent contributions at moderate to low levels.

Table 5. Summary of the top contributing variables in the study's M2 and MC time series. Variables are ordered first by the number of times the variable appeared in the final models of the eight, five-year intervals of the triplicated times series (n), followed by the variable's mean permutation importance (PI) ± standard error across those appearances.

Variable	n	PI	Description
M2 time series			
SPEED	24	18.3 ± 1.7	Surface wind speed (m/s)
EVPSOIL	24	12.4 ± 1.9	Bare soil evaporation energy flux (W/m^2)
QV2M	24	6.2 ± 1.2	2-meter specific humidity (kg/kg)
EVPINTR	20	19.3 ± 1.5	Interception loss energy flux (W/m^2)
TAUTOT	17	9.9 ± 1.8	Optical thickness of all clouds
PREVTOT	15	16.4 ± 2.9	Total re-evaporation/sublimation of precipitation ($(kg/m^2)/s$)
SWGNT	13	20.8 ± 2.8	Surface net downward shortwave flux (W/m^2)
MC time series			
MC_Bio08	24	39.6 ± 3.1	Mean temperature of the wettest quarter (°C)
MC_Bio14	19	11.1 ± 1.0	Precipitation of the driest month (mm)
MC_Bio18	18	23.2 ± 2.9	Precipitation of the warmest quarter (mm)
MC_Bio03	16	10.7 ± 2.0	Isothermality [(MC_Bio2/MC_Bio07)*100] (%)
MC_Bio15	15	10.6 ± 1.3	Precipitation seasonality (Coefficient of variation) (%)
MC_Bio05	15	9.2 ± 3.7	Maximum temperature of the warmest month (°C)
MC_Bio13	12	8.1 ± 2.6	Precipitation of the wettest month (mm)

DISCUSSION

Complex 40-year patterns of changing climatic suitability

Velocity of change consistent with other findings

The shifts in favorable conditions we observed across both time series are consistent with what has been reported for Cassin's Sparrow and many other North American grassland bird species (Bateman et al. 2016, Huang et al. 2023). Bateman et al. (2016), for example, found an average bioclimatic velocity of 1.27 km/yr to the west, northwest, and north over the past 60 years in the potential breeding distributions of 285 species of land birds across the Continental U.S., with some potential breeding populations shifting at rates of up to 5.51 km/yr. Likewise, a recent study by Huang et al. (2023) reported a mean bioclimatic velocity of 2.25

Fig. 5. Maps showing the Theil-Sen trends for the top contributing variables in the M2 and MC time series, as shown in Table 5. Positive trends are shown in green; negative trends are shown in red. Color intensity represents the rate of change in the units of measure for the variable per five-year interval across the 40-year time series.

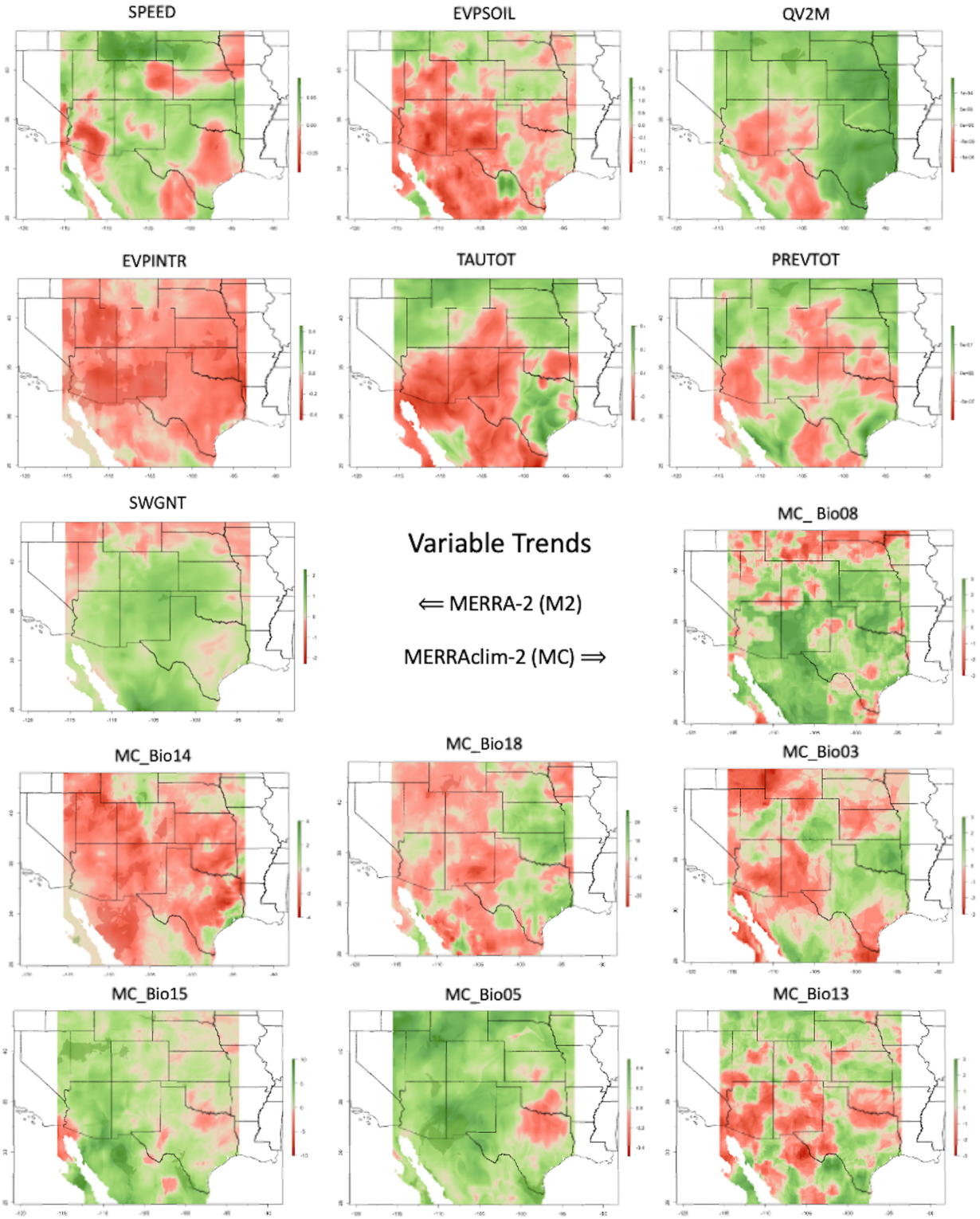

Table 6. Theil-Sen trend analysis of the top contributing variables in the study's M2 and MC time series. Positive (Pos) and negative (Neg) trend coverage areas represent the trend proportion across the entire study area and are calculated for the map regions in Figure 5 that exhibited overall change at any level of statistical significance.

M2 variable		% of area	MC variable		% of area
SPEED	Pos	62.5	MC_Bio08	Pos	67.5
	Neg	29.8		Neg	25.5
EVPSOIL	Pos	34.4	MC_Bio14	Pos	17.2
	Neg	63.1		Neg	73.3
QV2M	Pos	75.0	MC_Bio18	Pos	36.5
	Neg	22.3		Neg	62.1
EVPINTR	Pos	5.0	MC_Bio03	Pos	44.4
	Neg	76.7		Neg	53.4
TAUTOT	Pos	46.1	MC_Bio15	Pos	80.0
	Neg	53.4		Neg	14.8
PREVTOT	Pos	57.5	MC_Bio05	Pos	85.6
	Neg	41.7		Neg	7.9
SWGNT	Pos	79.5	MC_Bio13	Pos	54.6
	Neg	20.4		Neg	43.7

km/yr in 29 species of grassland birds along predominantly east-west axes of increasing environmental suitability, accompanied by an estimated, mean abundance-based velocity of 5.02 km/yr along more northerly inclined axes of increasing abundance.

Trends and patterns of change vary across time series

Our two time series reveal contrasting histories of climatic suitability change over the past 40 years. The MC time series paints a more favorable picture of changing conditions than what is seen in the M2 time series, with areas of overall improving conditions exceeding areas of declining conditions by 45.1% in the former and only 14.8% in the latter (Table 4). This contrast in overall trend is particularly apparent across the western regions of the study area and within the USGS GAP boundaries of Cassin's Sparrow's northernmost breeding range (Figs. 2B, 3B). In the west, M2-driven model results portray a northerly shift in improving conditions across the full extent of the study area. With the MC-driven models, changes are not nearly as distinct nor are they as extensive. The M2-driven model results show sharply improving climatic suitability in the northeastern extent of the breeding range and a fall-off along the western boundaries of Cassin's Sparrow's breeding and non-breeding ranges, whereas the MC-driven model results show improving climatic suitability in the northeastern region and a fall-off along the western boundary of only Cassin's Sparrow's non-breeding range.

State-level scale highlights differing trends and patterns

The differences between the two time series become more noticeable when results are considered at the state level. Cassin's Sparrow's breeding and non-breeding ranges comprise seven states within the Continental U.S.: Arizona (AZ), Colorado (CO), Kansas (KS), Nebraska (NE), New Mexico (NM), Oklahoma (OK), and Texas (TX) (Figs. 2B, 3B). Cassin's Sparrow is found in four of these states only during the breeding season (i.e., CO, KS, NE, and OK). With KS and OK, we see similar trend patterns across the two time series. On the other hand, for CO, we see a sharp decline in suitability in the M2 time series, especially in the central part of the state, and a general improvement in conditions in the MC series. We see the inverse pattern for NE across the two series, with the decline in the MC series in the north-central part of the state.

Within the U.S., Cassin's Sparrow has historically been most abundant in AZ, NM, and TX (North American breeding bird survey, https://www.pwrc.usgs.gov/bbs/). These states represent the heart of Cassin's Sparrow's U.S. range, and it is here we see the most striking differences in the M2 and MC time series' model results. In the M2 series, climatic suitability in areas that historically accommodated seasonal range expansion between non-breeding and breeding seasons is shown to have been declining over the past 40 years in AZ and NM. In contrast, climatic suitability in these areas appears to be improving or largely unchanged in the MC series. In TX, M2 model results indicate improving breeding season conditions in northern regions and decreasing suitability along the state's southern border in breeding and non-breeding areas; similar but less pronounced patterns are observed in the MC time series.

Implications for conservation practice

The variability we see across the two time series and across the species' geographic range has practical implications for conservation policy development and implementation. Population size, species abundance, and similar attributes are a central component of essentially all state-level conservation status formulation processes (Association of Fish and Wildlife Agencies State Wildlife Actions Plans, https://www.fishwildlife.org). It has been shown that the combination of bioclimatic predictors with other environmental attributes, such as ecosystem functional attributes, edaphic variables, topographic data, vegetation indices, and microclimatic variables, can capture factors affecting abundance rather than just occurrence, thereby yielding suitability model results that are often highly correlated with abundance (Cabello et al. 2012, Weber et al. 2017, Leitão and Santos 2019, Regos et al. 2020, Arenas-Castro and Sillero 2021, Cavalcante et al. 2022). In our results, we see that patterns of historical change in environmental suitability can vary widely depending on the spatial extent considered and on whether time series models are driven by bioclimatic variables alone or by variables more aligned with ecosystem functioning. It is possible that our results are an indicator that demographic and other observational survey results may vary greatly across the species' range as well, which could lead to differing conclusions regarding the conservation status of Cassin's Sparrow and possibly account for the inconsistencies we observe in the literature and among states regarding this species' status.

Complex 40-year patterns of changing environmental drivers

Drought and seasonal precipitation are important macroclimatic drivers

The MC time series provides insights into how climatic changes have influenced seasonal trends that are important to Cassin's Sparrow (Table 5). The three most contributory variables in the MC time series are mean temperature of the wettest quarter (MC_Bio08), which appears to have been generally increasing across Cassin's Sparrow's range over the past 40 years while declining in importance as an environmental driver; total precipitation of the driest month (MC_Bio14), which has been decreasing across Cassin's Sparrow's range while increasing in importance as an environmental driver over the same period of

Fig. 6. Diagrams showing the relative importance of the top contributing variables across the five-year intervals of the M2 (left) and MC (right) time series over the 40-year span of the study. The variables named in the first column of each diagram are listed in descending order of their overall contribution to the time series, as shown in Table 5. The colored lines associated with each variable show how the relative importance of the variables changed over the 40-year span of the study. These trends in relative importance provide clues to the environmental factors driving Cassin's Sparrow's biological response to changing climatic conditions, as described in the accompanying text.

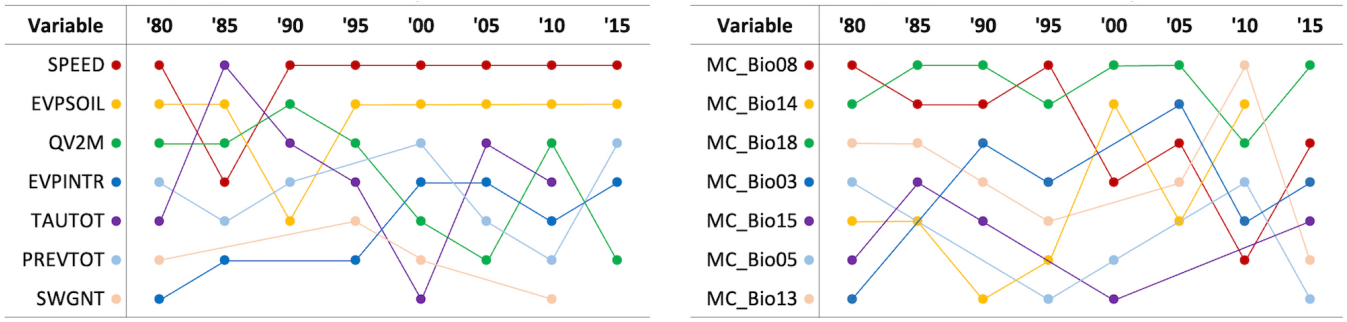

time; and precipitation of the warmest quarter (MC_Bio18), which has also been generally decreasing across the species' range but displays a discontinuous patchwork of positive and negative trends while remaining one of the top environmental drivers over the 40-year span of the study. Collectively, these three variables appear to confirm that the long-running drought conditions across southwestern North America have had a major influence on climatic suitability for Cassin's Sparrow (Stahle 2020, Williams et al. 2020). That MC_Bio18 is consistently the most important variable across the time series is notable, given that this variable essentially characterizes the seasonal precipitation pattern of the North American Monsoon (Adams and Comrie 1997, Becker 2021). The next two most contributory variables are isothermality (MC_Bio03) and precipitation seasonality (MC_Bio15). The consistent contribution of these two variables to the MC time series suggests that variability in both temperature levels and precipitation amounts has also had a historical influence on climatic suitability for Cassin's Sparrow.

Wind speed and drying soils are important microclimatic drivers

The M2 time series provides insights into how trends in ground-level factors have influenced environmental suitability for Cassin's Sparrow (Table 5). The two most important variables in the M2 time series are surface wind speeds (SPEED), which appears to have been generally increasing across the study area over the past 40 years while remaining a consistently top model contributor, and bare soil evaporation energy flux (EVPSOIL), which is generally decreasing across the study area over this period, especially in the southwestern region, while also remaining a top contributor across the time series. Wind has a mixing effect on air near the ground that can increase the evaporation of water from soil and plant surfaces until a point is reached where drying conditions take over (Tran et al. 2016, Lian et al. 2022). Further evidence of this phenomenon is seen in the water loss from plant surfaces, as reflected by interception loss energy flux (EVPINTR), the fourth most contributory variable, which has been decreasing over the past 40 years while its importance as a driver in our models has steadily increased. Total re-evaporation of precipitation (PREVTOT), which can contribute to reduced precipitation efficiency (i.e., the amount of falling precipitation that evaporates or sublimates before reaching the ground), is the sixth most contributory variable. In our results, there has been a generally increasing trend in PREVTOT across much of the study area while the driver itself has remained moderately consistent in importance across the 40-year span of the study. These factors, along with increasing shortwave radiant energy from the sun (SWGNT) and decreasing cloud thickness (TAUTOT), the seventh and fifth most important variables, respectively, appear to be contributing to decreasing water content of the atmosphere (QV2M) across the North American Southwest. Our results indicate that QV2M itself, the third most important contributory variable overall, has decreased in importance as an environmental driver over the years as SPEED, EVPSOIL, and EVPINTR have become the dominant influences. Taken together, however, the higher surface wind speeds, reduced bare soil evaporation, drying air, and lower precipitation efficiency reflected in the M2 time series' top four variables suggest that microclimatic drying may be the particular aspect of varying monsoon precipitation of importance to Cassin's Sparrow (Tran et al. 2016, Lehmann et al. 2018, Cheng et al. 2021, Lian et al. 2022, Peevey 2022).

Implications for future status assessments

The observed connection between top contributing variables, monsoon rainfall, and ground-level drying conditions is consistent with what is known about Cassin's Sparrow's ground-dwelling habit and the importance of microclimatic conditions to almost all aspects of the species' life (Schnase and Maxwell 1989, Schnase et al. 1991). Our results are also consistent with research showing that increasing temperatures, increased temperature and precipitation variability, and drying soils are potent drivers of environmental suitability for many species found across the arid grasslands of the southwestern U.S. (Varner and Dearing 2014, Lortie et al. 2022). All told, it appears that spatiotemporal attributes of North American monsoon precipitation; variables related to the surface moisture conditions of the soil, air, and vegetation; and surface wind speed should be considered variables of particular relevance to Cassin's Sparrow and perhaps key to understanding the species' conservation status. It is important to note, however, that large-scale inferences are often complicated by changing properties in the underlying processes that drive phenomena, such as the spatially and temporally varying trends we see in the M2 and MC variables (Rollinson et al. 2021). As a

result, Cassin's Sparrow's response to these non-constant trends tends to be complex and localized, which limits our ability to generalize about widespread trends in overall conditions that may be influencing the species.

CONCLUSION

We have used an automated and reproducible approach to retrospective ENM to better understand historical patterns of changing climatic suitability for Cassin's Sparrow, the key drivers underlying the species' response to a changing climate, and whether that response might contribute to the variability we see across various status assessments for the species. To do this, we built two multi-decadal, time- and variable-specific MaxEnt time series based on NASA's MERRA-2 reanalysis. Trend analysis of the MC time series provided a seasonal, macroclimatic perspective that confirmed the importance of monsoon rainfall in Cassin's Sparrow's response to changing environmental conditions. Trend analysis of the M2 time series provided a microclimatic view that revealed the importance of increasing wind speed and drying land surface conditions to the species' response. Estimates of climatic suitability for Cassin's Sparrow in the MC time series were generally more favorable than what we observed in the M2 time series. The differences between the two time series were even more pronounced when considered at the state level. These two findings could have important implications for conservation practice, given that the vast majority of conservation policy decisions and management actions play out at the state level and often rely heavily on climatic suitability models based solely on bioclimatic predictors. Furthermore, our results suggest that modeled estimates of climatic suitability for Cassin's Sparrow can vary widely depending on the temporal frame, spatial extent, and environmental drivers considered. This likely reflects Cassin's Sparrow's localized response to non-constant, spatiotemporal trends in the drivers themselves. This variability mirrors the inconsistencies we see in the current literature regarding this species' status and points to the need for an updated, state-by-state examination of Cassin's Sparrow's regional vulnerabilities. Given the variability we observed in climatic suitability across areas occupied by Cassin's Sparrow during the breeding season, a closer look at the nature and scope of historical, inter-annual range changes and local population trends would also be helpful in clarifying the relationship between climatic suitability and the demographic status of the species. Retrospective ENM that incorporates both time and variable specificity, as we have done here, appears to be a promising approach to understanding the complexities of a species' response to changing climatic conditions and a useful adjunct to assessments of a species' conservation status.

Author Contributions:

JLS: conceptualization, formal analysis, investigation, methodology, software, writing – original draft. MLC: conceptualization, formal analysis, methodology, writing – review & editing. PMM, VAS: formal analysis, writing – review & editing.

Acknowledgments:

The authors wish to thank our subject editor and two anonymous reviewers for helpful comments on earlier versions of the manuscript. We thank our NASA Innovation Lab colleagues for their many contributions and ongoing technical support of these efforts. Resources supporting this work were provided by the NASA High-End Computing (HEC) Program through the NASA Center for Climate Simulation (NCCS) at Goddard Space Flight Center.

Data Availability:

The data and code that support the findings of this study are openly available in GitHub at https://github.com/jschnase/MMX_Toolkit.

LITERATURE CITED

Adams, D. K., and A. C. Comrie. 1997. The North American monsoon. Bulletin of the American Meteorological Society 78:2197-2213. https://doi.org/10.1175/1520-0477(1997)078<2197:TNAM>2.0.CO;2

Aiello-Lammens, M. E., R. A. Boria, A. Radosavljevic, B. Vilela, and R. P. Anderson. 2015. spThin: an R package for spatial thinning of species occurrence records for use in ecological niche models. Ecography 38(5):541-545. https://doi.org/10.1111/ecog.01132

Akaike, H. 1974. A new look at the statistical model identification. IEEE Transactions on Automatic Control 19(6):716-723. https://doi.org/10.1109/TAC.1974.1100705

Allouche, O., A. Tsoar, and R. Kadmon. 2006. Assessing the accuracy of species distribution models: prevalence, kappa and the true skill statistic (TSS). Journal of Applied Ecology 43 (6):1223-1232. https://doi.org/10.1111/j.1365-2664.2006.01214.x

Arenas-Castro, S., J. Gonçalves, P. Alves, D. Alcaraz-Segura, and J. P. Honrado. 2018. Assessing the multi-scale predictive ability of ecosystem functional attributes for species distribution modelling. PLoS ONE 13(6):e0199292. https://doi.org/10.1371/journal.pone.0199292

Arenas-Castro, S., and N. Sillero. 2021. Cross-scale monitoring of habitat suitability changes using satellite time series and ecological niche models. Science of The Total Environment 784:147172. https://doi.org/10.1016/j.scitotenv.2021.147172

Bateman, B. L., A. M. Pidgeon, V. C. Radeloff, J. VanDerWal, W. E. Thogmartin, S. J. Vavrus, and P. J. Heglund. 2016. The pace of past climate change vs. potential bird distributions and land use in the United States. Global Change Biology 22:1130-1144. https://doi.org/10.1111/gcb.13154

Becker, E. 2021. The North American Monsoon. ENSO Blog. https://www.climate.gov/news-features/blogs/enso/north-american-monsoon

Bede-Fazekas, Á., and I. Somodi. 2020. The way bioclimatic variables are calculated has impact on potential distribution models. Methods in Ecology and Evolution 11(2):1559-1570. https://doi.org/10.1111/2041-210X.13488

Boria, R. A., L. E. Olson, S. M. Goodman, and R. P. Anderson. 2014. Spatial filtering to reduce sampling bias can improve the performance of ecological niche models. Ecological Modelling 275:73-77. https://doi.org/10.1016/j.ecolmodel.2013.12.012

Bosilovich, M. G., R. Lucchesi, and M. Suarez. 2016. MERRA-2: file specification. NASA Global Modeling and Assimilation Office Note No. 9 (Version 1.1). NASA Goddard Space Flight Center, Greenbelt, Maryland, USA. https://gmao.gsfc.nasa.gov/pubs/docs/Bosilovich785.pdf

Cabello, J., N. Fernández, D. Alcaraz-Segura, C. Oyonarte, G. Piñeiro, A. Altesor, M. Delibes, and J. M. Paruelo. 2012. The ecosystem functioning dimension in conservation: insights from remote sensing. Biodiversity and Conservation 21:3287-3305. https://doi.org/10.1007/s10531-012-0370-7

Cavalcante, T., M. M. Weber, and A. A. Barnett. 2022. Combining geospatial abundance and ecological niche models to identify high-priority areas for conservation: the neglected role of broadscale interspecific competition. Frontiers in Ecology and Evolution 10:915325. https://doi.org/10.3389/fevo.2022.915325

Cheng, Y., P. W. Chan, X. Wei, Z. Hu, Z. Kuang, and K. A. McColl. 2021. Soil moisture control of precipitation reevaporation over a heterogeneous land surface. Journal of the Atmospheric Sciences 78:3369-3383. https://doi.org/10.1175/JAS-D-21-0059.1

Dunning, J. B., R. K. Bowers, Jr., S. J. Suter, and C. E. Bock. 2020. Cassin's Sparrow (*Peucaea cassinii*) version 1.0. In P. G. Rodewald, editor. Birds of the world. Cornell Lab of Ornithology, Ithaca, New York, USA. https://doi.org/10.2173/bow.casspa.01

Edwards, P. N. 2010. A vast machine: computer models, climate data, and the politics of global warming. MIT Press, Cambridge, Massachusetts, USA.

Elith, J., S. J. Phillips, T. Hastie, M. Dudík, Y. E. Chee, and C. J. Yates. 2011. A statistical explanation of MaxEnt for ecologists. Diversity and Distributions 17:43-57. https://doi.org/10.1111/j.1472-4642.2010.00725.x

Fielding, A. H., and J. F. Bell. 1997. A review of methods for the assessment of prediction errors in conservation presence/absence models. Environmental Conservation 24(1):38-49. https://doi.org/10.1017/S0376892997000088

Gelaro, R., W. McCarty, M. J. Suárez, R. Todling, A. Molod, L. Takacs, C. A. Randles, A. Darmenov, M. G. Bosilovich, R. Reichle, et al. 2017. The modern-era retrospective analysis for research and applications, version 2 (MERRA-2). Journal of Climate 30:5419-5454. https://doi.org/10.1175/JCLI-D-16-0758.1

Goberville, E., G. Beaugrand, N.-C. Hautekèete, Y. Piquot, and C. Luczak. 2015. Uncertainties in the projection of species distributions related to general circulation models. Ecology and Evolution 5(5):1100-1116. https://doi.org/10.1002/ece3.1411

Gonçalves, J., P. Alves, I. Pôças, B. Marcos, R. Sousa-Silva, Â. Lomba, and J. P. Honrado. 2016. Exploring the spatiotemporal dynamics of habitat suitability to improve conservation management of a vulnerable plant species. Biodiversity and Conservation 25:2867-2888. https://doi.org/10.1007/s10531-016-1206-7

Guida, R. J., S. R. Abella, C. L. Roberts, C. M. Norman, and W. J. Smith, Jr. 2019. Assessing historical and future habitat models for four conservation-priority Mojave Desert species. Journal of Biogeography 46:2081-2097. https://doi.org/10.1111/jbi.13645

Guisan, A., R. Tingley, J. B. Baumgartner, I. Naujokaitis-Lewis, P. R. Sutcliffe, A. I. T. Tulloch, T. J. Regan, L. Brotons, E. McDonald-Madden, C. Mantyka-Pringle, et al. 2013. Predicting species distributions for conservation decisions. Ecology Letters 16:1424-1435. https://doi.org/10.1111/ele.12189

Heenan, C. B., and R. S. Seymour. 2012. The effect of wind on the rate of heat loss from avian cup-shaped nests. PLoS ONE 7 (2):e32252. https://doi.org/10.1371/journal.pone.0032252

Hijmans, R. J., S. Phillips, J. Leathwick, and J. Elith. 2023. dismo: species distribution modeling. R package version 1.3-1.4. https://cran.r-project.org/web/packages/dismo/index.html

Huang, Q., B. L. Bateman, N. L. Michel, A. M. Pidgeon, V. C. Radeloff, P. Heglund, A. J. Allstadt, A. J. Nowakowski, J. Wong, and J. R. Sauer. 2023. Modeled distribution shifts of North American birds over four decades based on suitable climate alone do not predict observed shifts. Science of The Total Environment 857(3):159603. https://doi.org/10.1016/j.scitotenv.2022.159603

Hubbard, J. P. 1974. Avian evolution in the aridlands of North America. Living Bird 12:155-196.

Huntley, B., P. Barnard, R. Altwegg, L. Chambers, B. W. T. Coetzee, L. Gibson, P. A. R. Hockey, D. G. Hole, G. F. Midgley, L. G. Underhill, and S. G. Willis. 2010. Beyond bioclimatic envelopes: dynamic species' range and abundance modelling in the context of climatic change. Ecography 33:621-626. https://doi.org/10.1111/j.1600-0587.2009.06023.x

Iknayan, K. J., and S. R. Beissinger. 2018. Collapse of a desert bird community over the past century driven by climate change. Proceedings of the National Academy of Sciences 115 (34):8597-8602. https://doi.org/10.1073/pnas.1805123115

Ingenloff, K. 2020. Enhancing the correlative ecological niche modeling framework to incorporate the temporal dimension of species' distributions. Dissertation. University of Kansas, Lawrence, Kansas, USA. https://www.proquest.com/openview/56e595f00e55b6ffa8cf92c702a3dc96/1?pq-origsite=gscholar&cbl=18750&diss=y

Ingenloff, K., and A. T. Peterson. 2021. Incorporating time into the traditional correlational distributional modelling framework: a proof-of-concept using the Wood Thrush *Hylocichla mustelina*. Methods in Ecology and Evolution 12:311-321. https://doi.org/10.1111/2041-210X.13523

Johnston, A., T. Auer, D. Fink, M. Strimas-Mackey, M. Iliff, K. V. Rosenberg, S. Brown, R. Lanctot, A. D. Rodewald, and S. Kelling. 2020. Comparing abundance distributions and range maps in spatial conservation planning for migratory species. Ecological Applications 30(3):02058. https://doi.org/10.1002/eap.2058

Kalinski, C. E. 2019. Building better species distribution models with machine learning: assessing the role of covariate scale and tuning in Maxent models. Dissertation. University of Southern California, Los Angeles, California, USA.

Kass, J. M., R. Muscarella, P. J. Galante, C. Bohl, G. E. Buitrago-Pinilla, R. A. Boria, M. Soley-Guardia, and R. P. Anderson. 2023. ENMeval: automated tuning and evaluations of ecological niche models. R package version 2.0.4. https://cran.r-project.org/web/packages/ENMeval/index.html

Lehmann, P., O. Merlin, P. Gentine, and D. Or. 2018. Soil texture effects on surface resistance to bare-soil evaporation. Geophysical Research Letters 45(19):10398-10405. https://doi.org/10.1029/2018GL078803

Leitão, P. J., and M. J. Santos. 2019. Improving models of species ecological niches: a remote sensing overview. Frontiers in Ecology and Evolution 7:9. https://doi.org/10.3389/fevo.2019.00009

Lian, X., W. Zhao, and P. Gentine. 2022. Recent global decline in rainfall interception loss due to altered rainfall regimes. Nature Communications 13:7642. https://doi.org/10.1038/s41467-022-35414-y

Lipschutz, M. L. 2016. Effects of drought and grazing on land bird populations in South Texas. Dissertation. Texas A&M University-Kingsville, Kingsville, Texas, USA. https://www.proquest.com/dissertations-theses/effects-drought-grazing-on-land-bird-populations/docview/1814764436/se-2

Lortie, C. J., A. Filazzola, M. Westphal, and H. S. Butterfield. 2022. Foundation plant species provide resilience and microclimatic heterogeneity in drylands. Scientific Reports 12:18005. https://doi.org/10.1038/s41598-022-22579-1

Lynn, J. 2006. Cassin's Sparrow (*Aimophila cassinii*): a technical conservation assessment. U.S. Department of Agriculture Forest Service, Rocky Mountain Region, Lakewood, Colorado, USA. https://www.fs.usda.gov/Internet/FSE_DOCUMENTS/stelprdb5182053.pdf

Maguire, B., Jr. 1973. Niche response structure and the analytical potentials of its relationship to the habitat. American Naturalist 107:213-246. https://doi.org/10.1086/282827

Merow, C., M. J. Smith, and J. A. Silander, Jr. 2013. A practical guide to MaxEnt for modeling species' distributions: what it does, and why inputs and settings matter. Ecography 36(10):1058-1069. https://doi.org/10.1111/j.1600-0587.2013.07872.x

Muscarella, R., P. J. Galante, M. Soley-Guardia, R. A. Boria, J. M. Kass, M. Uriarte, and R. P. Anderson. 2014. ENMeval: an R package for conducting spatially independent evaluations and estimating optimal model complexity for Maxent ecological niche models. Methods in Ecology and Evolution 5(11):1198-1205. https://doi.org/10.1111/2041-210X.12261

New Mexico Department of Game and Fish. 2016. State wildlife action plan for New Mexico. New Mexico Department of Game and Fish, Santa Fe, New Mexico, USA. https://www.wildlife.state.nm.us/wpfb-file/new-mexico-state-wildlife-action-plan-swap-final-2019-pdf

Norman, J. A., and L. Christidis. 2016. Ecological opportunity and the evolution of habitat preferences in an arid-zone bird: implications for speciation in a climate-modified landscape. Scientific Reports 6:19613. https://doi.org/10.1038/srep19613

O'Donnell, M. S., and D. A. Ignizio. 2012. Bioclimatic predictors for supporting ecological applications in the conterminous United States. U.S. Geological Survey Data Series 691. U.S. Geological Survey, Reston, Virginia, USA. https://doi.org/10.3133/ds691

Ohmart, R. D. 1969. Dual breeding ranges in Cassin's Sparrow (*Aimophila cassinii*). Page 105 in C. C. Hoff and M. L. Riedesel, editors. Physiological systems in semiarid environments. University of New Mexico Press, Albuquerque, New Mexico, USA.

Pearson, R. G., C. J. Raxworthy, M. Nakamura, and A. Townsend Peterson. 2007. Predicting species distributions from small numbers of occurrence records: a test case using cryptic geckos in Madagascar. Journal of Biogeography 34:102-117. https://doi.org/10.1111/j.1365-2699.2006.01594.x

Pecl, G. T., M. B. Araújo, J. D. Bell, J. Blanchard, T. C. Bonebrake, I.-C. Chen, T. D. Clark, R. K. Colwell, F. Danielsen, B. Evengård, et al. 2017. Biodiversity redistribution under climate change: impacts on ecosystems and human well-being. Science 355: eaai9214. https://doi.org/10.1126/science.aai9214

Peevey, T. 2022. Changes in US wind speeds since 2000 point to a dynamic landscape. https://www.spglobal.com/marketintelligence/en/news-insights/research/changes-in-us-wind-speeds-since-2000-point-to-a-dynamic-landscape

Pérez-Navarro, M. A., O. Broennimann, M. A. Esteve, J. M. Moya-Perez, M. F. Carreño, A. Guisan, and F. Lloret. 2021. Temporal variability is key to modelling the climatic niche. Diversity and Distributions 27:473-484. https://doi.org/10.1111/ddi.13207

Peterson, A. T., J. Soberón, R. G. Pearson, R. P. Anderson, E. Martínez-Meyer, M. Nakamura, and M. B. Araújo. 2011. Ecological niches and geographic distributions (MPB-49). Princeton University Press, Princeton, New Jersey, USA. https://doi.org/10.23943/princeton/9780691136868.001.0001

Petitpierre, B., O. Broennimann, C. Kueffer, C. Daehler, and A. Guisan. 2017. Selecting predictors to maximize the transferability of species distribution models: lessons from cross-continental plant invasions. Global Ecology and Biogeography 26:275-287. https://doi.org/10.1111/geb.12530

Pettorelli, N., H. Schulte to Bühne, A. Tulloch, G. Dubois, C. Macinnis-Ng, A. M. Queirós, D. A. Keith, M. Wegmann, F. Schrodt, M. Stellmes, et al. 2018. Satellite remote sensing of ecosystem functions: opportunities, challenges and way forward. Remote Sensing in Ecology and Conservation 4(2):71-93. https://doi.org/10.1002/rse2.59

Phillips, S. J., R. P. Anderson, M. Dudík, R. E. Schapire, and M. E. Blair. 2017. Opening the black box: an open-source release of Maxent. Ecography 40(7):887-893. https://doi.org/10.1111/ecog.03049

Phillips, S. J., R. P. Anderson, and R. E. Schapire. 2006. Maximum entropy modeling of species geographic distributions. Ecological Modelling 190(3-4):231-259. https://doi.org/10.1016/j.ecolmodel.2005.03.026

Porzig, E. L., N. E. Seavy, T. Gardali, G. R. Geupel, M. Holyoak, and J. M. Eadie. 2014. Habitat suitability through time: using time series and habitat models to understand changes in bird density. Ecosphere 5:12. https://doi.org/10.1890/ES13-00166.1

Pradhan, P. 2016. Strengthening MaxEnt modelling through screening of redundant explanatory bioclimatic variables with variance inflation factor analysis. Researcher 8(5):29-34. https://www.academia.edu/28906048/Strengthening_MaxEnt_modelling_through_screening_of_redundant_explanatory_Bioclimatic_Variables_with_Variance_Inflation_Factor_analysis

Regos, A., P. Gómez-Rodríguez, S. Arenas-Castro, L. Tapia, M. Vidal, and J. Domínguez. 2020. Model-assisted bird monitoring based on remotely sensed ecosystem functioning and atlas data. Remote Sensing 12:2549. https://doi.org/10.3390/rs12162549

Regos, A., J. Gonçalves, S. Arenas-Castro, D. Alcaraz-Segura, A. Guisan, and J. P. Honrado. 2022a. Mainstreaming remotely sensed ecosystem functioning in ecological niche models. Remote Sensing in Ecology and Conservation 8(4):431-447. https://doi.org/10.1002/rse2.255

Regos, A., L. Tapia, S. Arenas-Castro, A. Gil-Carrera, and J. Domínguez. 2022b. Ecosystem functioning influences species fitness at upper trophic levels. Ecosystems 25:1037-1051. https://doi.org/10.1007/s10021-021-00699-5

Reside, A. E., J. J. VanDerWal, A. S. Kutt, and G. C. Perkins. 2010. Weather, not climate, defines distributions of vagile bird species. PLoS ONE 5(10):e13569. https://doi.org/10.1371/journal.pone.0013569

Rollinson, C. R., A. O. Finley, M. R. Alexander, S. Banerjee, K.-A. Dixon Hamil, L. E. Koenig, D. H. Locke, M. L. DeMarche, M. W. Tingley, K. Wheeler, et al. 2021. Working across space and time: nonstationarity in ecological research and application. Frontiers in Ecology and the Environment 19(1):66-72. https://doi.org/10.1002/fee.2298

Rosenberg, K. V., A. M. Dokter, P. J. Blancher, J. R. Sauer, A. C. Smith, P. A. Smith, J. C. Stanton, A. Panjabi, L. Helft, M. Parr, and P. P. Marra. 2019. Decline of the North American avifauna. Science 366(6461):120-124. https://doi.org/10.1126/science.aaw1313

Rosenberg, K. V., J. A. Kennedy, R. Dettmers, R. P. Ford, D. Reynolds, J. D. Alexander, C. J. Beardmore, P. J. Blancher, R. E. Bogart, G. S. Butcher, et al. 2016. Partners in Flight landbird conservation plan: 2016 revision for Canada and continental United States. https://partnersinflight.org/resources/the-plan/

Roubicek, A. J., J. VanDerWal, L. J. Beaumont, A. J. Pitman, P. Wilson, and L. Hughes. 2010. Does the choice of climate baseline matter in ecological niche modelling? Ecological Modelling 221 (19):2280-2286. https://doi.org/10.1016/j.ecolmodel.2010.06.021

Ruth, J. M. 2000. Cassin's Sparrow (*Aimophila cassinii*) status assessment and conservation plan. U.S. Fish and Wildlife Service Biological Technical Publication BTP-R6002-2000. U.S. Geological Survey Midcontinent Ecological Science Center, Fort Collins, Colorado, USA. https://digitalmedia.fws.gov/digital/collection/document/id/1235/rec/4

Salas, E. A. L., V. A. Seamster, K. G. Boykin, N. M. Harings, and K. W. Dixon. 2017. Modeling the impacts of climate change on Species of Concern (birds) in South Central U.S. based on bioclimatic variables. AIMS Environmental Science 4(2):358-385. https://doi.org/10.3934/environsci.2017.2.358

Schnase, J. L., and M. L. Carroll. 2022. Automatic variable selection in ecological niche modeling: a case study using Cassin's Sparrow (*Peucaea cassinii*). PLoS ONE 17(1):e0257502. https://doi.org/10.1371/journal.pone.0257502

Schnase, J. L., M. L. Carroll, R. L. Gill, G. S. Tamkin, J. Li, S. L. Strong, T. P. Maxwell, M. E. Aronne, and C. S. Spradlin. 2021. Toward a Monte Carlo approach to selecting climate variables in MaxEnt. PLoS ONE 16(3):e0237208. https://doi.org/10.1371/journal.pone.0237208

Schnase, J. L., W. E. Grant, T. C. Maxwell, and J. J. Leggett. 1991. Time and energy budgets of Cassin's Sparrow (*Aimophila cassinii*) during the breeding season: evaluation through modelling. Ecological Modelling 55(3-4):285-319. https://doi.org/10.1016/0304-3800(91)90091-E

Schnase, J. L., and T. C. Maxwell. 1989. Use of song patterns to identify individual male Cassin's Sparrows. Journal of Field Ornithology 60(1):12-19. https://sora.unm.edu/sites/default/files/journals/jfo/v060n01/p0012-p0019.pdf

Searcy, C. A., and H. B. Shaffer. 2016. Do ecological niche models accurately identify climatic determinants of species ranges? American Naturalist 187(4):423-435. https://doi.org/10.1086/685387

Sen, P. K. 1968. Estimates of the regression coefficient based on Kendall's tau. Journal of the American Statistical Association 63 (324):1379-1389. https://doi.org/10.1080/01621459.1968.10480934

Smith, A. B., and M. J. Santos. 2020. Testing the ability of species distribution models to infer variable importance. Ecography 43 (12):1801-1813. https://doi.org/10.1111/ecog.05317

Sohl, T. L. 2014. The relative impacts of climate and land-use change on conterminous United States bird species from 2001 to 2075. PLoS ONE 9(11):e112251. https://doi.org/10.1371/journal.pone.0112251

Stahle, D. W. 2020. Anthropogenic megadrought. Science 368 (6488):238-239. https://doi.org/10.1126/science.abb6902

Theil, H. 1950. A rank-invariant method of linear and polynomial regression analysis. Indagationes Mathematicae 12:386-392. https://dwc.knaw.nl/DL/publications/PU00018789.pdf

Tran, D. T. Q., D. G. Fredlund, and D. H. Chan. 2016. Improvements to the calculation of actual evaporation from bare soil surfaces. Canadian Geotechnical Journal 53(1):118-133. https://doi.org/10.1139/cgj-2014-0512

VanDerWal, J., H. T. Murphy, A. S. Kutt, G. C. Perkins, B. L. Bateman, J. J. Perry, and A. E. Reside. 2013. Focus on poleward shifts in species' distribution underestimates the fingerprint of climate change. Nature Climate Change 3:239-243. https://doi.org/10.1038/nclimate1688

Varner, J., and M. D. Dearing. 2014. The importance of biologically relevant microclimates in habitat suitability assessments. PLoS ONE 9(8):e104648. https://doi.org/10.1371/journal.pone.0104648

Vega, G. C., L. R. Pertierra, and M. Á. Olalla-Tárraga. 2017. MERRAclim, a high-resolution global dataset of remotely sensed bioclimatic variables for ecological modelling. Scientific Data 4:170078. https://doi.org/10.1038/sdata.2017.78

Ward, E. J., L. A. K. Barnett, S. C. Anderson, C. J. C. Commander, and T. E. Essington. 2022. Incorporating non-stationary spatial variability into dynamic species distribution models. ICES Journal of Marine Science 79(9):2422-2429. https://doi.org/10.1093/icesjms/fsac179

Warren, D. L., and S. N. Seifert. 2011. Ecological niche modeling in Maxent: the importance of model complexity and the performance of model selection criteria. Ecological Applications 21(2):335-342. https://doi.org/10.1890/10-1171.1

Weber, M. M., R. D. Stevens, J. A. F. Diniz-Filho, and C. E. V. Grelle. 2017. Is there a correlation between abundance and environmental suitability derived from ecological niche modelling? A meta-analysis. Ecography 40(7):817-828. https://doi.org/10.1111/ecog.02125

Williams, A. P., E. R. Cook, J. E. Smerdon, B. I. Cook, J. T. Abatzoglou, K. Bolles, S. H. Baek, A. M. Badger, and B. Livneh. 2020. Large contribution from anthropogenic warming to an emerging North American megadrought. Science 368 (6488):314-318. https://doi.org/10.1126/science.aaz9600

Williams, F. C., and A. L. LeSassier. 1968. Cassin's Sparrow. Pages 981-990 in O. L. Austin, editor. Life histories of North American cardinals, grosbeaks, buntings, towhees, finches, sparrows, and allies, order Passeriformes, family Fringillidae: part 2, genera Pipilo through Spizella. Dover, New York, New York, USA.

Wilsey, C., L. Taylor, B. Bateman, C. Jensen, N. Michel, A. Panjabi, and G. Langham. 2019. Climate policy action needed to reduce vulnerability of conservation-reliant grassland birds in North America. Conservation Science and Practice 1(4):e21. https://doi.org/10.1111/csp2.21

Woodhouse, S. W. 1852. *Zonotrichia Cassinii*, nobis. Proceedings of the Academy of Natural Science of Philadelphia 60-61.

Appendix A. MERRA-2 (M2) variable definitions.*

M2T1NXSLV	**2D Atmospheric variables**
TS	Surface skin temperature (K) *– An approximation for the temperature of the Earth's tropopause, which lies about 17 km (11 miles) above the surface, expressed in degrees Kelvin. The tropopause is the boundary between the turbulent mixing-dominated troposphere and the more stable stratosphere.*
QV2M	2-meter specific humidity (kg/kg) *– The amount of water vapor contained in a unit amount of air, generally expressed as kg of water per kg of air.*
T2M	2-meter air temperature (K*)* *– The air temperature 2m above the ground, expressed in degrees Kelvin.*
M2T1NXFLX	**2D Surface fluxes**
EFLUX	Positive latent heat flux (W/m^2) *– The exchange of energy between the surface of the Earth and the atmosphere when water evaporates from or condenses onto the surface, expressed in Watts per square meter. Positive latent heat flux means that evaporation is occurring.*
HFLUX	Positive sensible heat flux (W/m^2) *– The exchange of energy between the surface of the Earth and the atmosphere when no state change is involved and energy is transferred by conduction, expressed in Watts per square meter. Positive sensible heat flux means heat is flowing from the surface to the atmosphere.*
SPEED	Surface wind speed (m/s) *– The speed of wind flow near the Earth's surface, expressed in meters per second.*

* These summaries were derived from definitions provided in: J. R. Holton, J. A. Curry, and J. A. Pyle, Eds., *Encyclopedia of atmospheric sciences*. Amsterdam; Boston: Academic Press, 2003. Details about the MERRA-2 collection and variable naming conventions can be found in in: Bosilovich, M.G., R. Lucchesi, and M. Suarez. 2016. "MERRA-2: File Specification." *GMAO Office Note* 9 (Version 1.1): 1–73.

PREVTOT — Total re-evaporation/sublimation of precipitation ([kg/m^2]/s)
– The amount of precipitation that evaporates (water to water vapor transition) or sublimates (snow or ice to water vapor transition) while falling through the atmosphere and fails to arrive at the land surface, expressed in mm per second. [1 kg of water spread over a square meter (kg/m^2) = 1 mm]

PRECTOTCORR — Total observation-corrected surface precipitation ([kg/m^2]/s)
– Total precipitation modeled from atmospheric physics corrected with satellite and/or gauge-based measurements, expressed in mm per second. [1 kg of water spread over a square meter (kg/m^2) = 1 mm]

M2T1NXRAD — 2D Surface and top-of-atmosphere radiation fluxes

ALBEDO — Surface albedo
– The amount of sunlight reflected by the Earth's surface, generally expressed as a decimal value with 1.0 being a perfect reflector and 0.0 absorbing all incoming light.

LWGNT — Surface net downward longwave flux (W/m^2)
– The rate of flow of radiant energy reaching the Earth's surface in the thermal infrared spectrum (4-100 μm), expressed in Watts per square meter. LWGNT is a result of atmospheric absorption, emission, and scattering within the entire atmospheric column.

SWGNT — Surface net downward shortwave flux (W/m^2)
– An estimate of the total amount of shortwave (0.3-4.0 μm) radiative energy that reaches the Earth's surface, expressed in Watts per square meter. SWGNT is an important source of energy and important influence on land-atmosphere and vegetation interactions, SWGNT has many applications in the general and applied sciences.

TAUTOT — Optical thickness of all clouds
– A measure of attenuation of the light passing through the atmosphere due to the scattering and absorption by cloud droplets. TAUTOT is a dimensionless, monotonically increasing function that approaches zero as cloud thickness approaches zero.

CLDTOT — Total cloud area fraction
– The proportion of the sky covered by all the visible clouds, an important influence on downward solar radiation.

M2T1NXLND 2D Land surface variables

LAI	Leaf area index *– A complex variable that relates the size of plant canopies to canopy density and the angle at which leaves are oriented to one another and to incident light. A dimensionless quality that is often used as an indicator of plant growth rate.*
GRN	Vegetation greenness fraction *– The proportion of ground covered by green vegetation. Values range from 0 to 1.*
GWETPROF	Average profile soil wetness *– The amount of water and water vapor present in the soil, generally expressed as the proportion of water present in a given volume of soil. Values range from 0 to 1.*
GWETROOT	Root zone soil wetness *– The amount of water and water vapor available to plants in the root zone, generally considered to be the upper 200 cm of soil, expressed as the proportion of water present in a given amount of soil. Values range from 0 to 1.*
TSURF	Mean land surface temperature (K) *– The radiative temperature of the Earth's land surface, expressed in degrees Kelvin.*
TSAT	Surface temperature of saturated zone (K) *– Surface temperature of soil in which all the interstices or voids are filled with groundwater, expressed in degrees Kelvin.*
FRWLT	Fractional wilting area *– Proportion of the land surface where the moisture content causes plants to wilt. Values range from 0 to 1.*
QINFIL	Soil water infiltration rate ([km/m^2]/s)) *– A measure of how fast water enters the soil, expressed in mm per second. [1 kg of water spread over a square meter (kg/m^2) = 1 mm]*
GHLAND	Downward heat flux into topsoil layer (W/m^2) *– The amount of thermal energy transferred to the soil, which can be affected by such factors as soil and air temperature, soil water content, canopy characteristics, and wind speed, expressed in Watts per square meter.*

WCHANGE Total land water change per unit time ([kg/m^2]/s)
– Total rate of movement of water to and from the Earth's surface, expressed in mm per second. [1 kg of water spread over a square meter (kg/m^2) = 1 mm].

ECHANGE Total land energy change per unit time (W/m^2)
– Total rate of energy transferred to and from the Earth's surface, expressed in Watts per square meter.

PRMC Total profile soil moisture content (m^3/m^3)
– The amount of water present in the soil, expressed as cubic meters of water per cubic meter of soil.

RZMC Root zone soil moisture content (m^3/m^3)
– The amount of water in the soil root zone, expressed as cubic meters of water per cubic meter of soil.

EVPSOIL Bare soil evaporation energy flux (W/m^2)
– The rate of radiant energy transfer when water evaporates from a saturated land surface, expressed in Watts per square meter.

EVPTRNS Transpiration energy flux (W/m^2)
– The amount of energy released as water evaporates at the plant leaf / atmosphere interface, expressed in Watts per square meter.

EVPINTR Interception loss energy flux (W/m^2)
– The portion of precipitation that is returned to the atmosphere through evaporation from plant surfaces or absorbed by plants and does not reach the ground, expressed in Watts per square meter.

EVLAND Evaporation from land ([kg/m^2]/s)
– The rate of moisture transfer from the land surface to the atmosphere, expressed in mm per second. [1 kg of water spread over a square meter (kg/m^2) = 1 mm]. Evapo-transpiration is the sum of all processes by which water moves from the land surface to the atmosphere via evaporation (EVLAND, EVPINTR, etc.) and transpiration (EVPTRNS).